Chemistry & Biology
Article

The E1 Mechanism in Photo-Induced β-Elimination Reactions for Green-to-Red Conversion of Fluorescent Proteins

Hidekazu Tsutsui,[1] Hideaki Shimizu,[2] Hideaki Mizuno,[1] Nobuyuki Nukina,[2] Toshiaki Furuta,[3] and Atsushi Miyawaki[1,*]
[1]Laboratory for Cell Function Dynamics
[2]Laboratory for Structural Neuropathology
Brain Science Institute, RIKEN, 2-1 Hirosawa, Wako-city, Saitama, 351-0198, Japan
[3]Department of Biomolecular Science, Research Center for Materials with Integrated Properties, Toho University, 2-2-1 Miyama, Funabashi, Chiba 274-8510, Japan
*Correspondence: matsushi@brain.riken.jp
DOI 10.1016/j.chembiol.2009.10.010

SUMMARY

KikGR is a fluorescent protein engineered to display green-to-red photoconvertibility that is induced by irradiation with ultraviolet or violet light. Similar to Kaede and EosFP, two naturally occurring photoconvertible proteins, KikGR contains a His^{62}-Tyr^{63}-Gly^{64} tripeptide sequence, which forms a green chromophore that can be photoconverted to a red one via formal β-elimination and subsequent extension of a π-conjugated system. Using a crystallizable variant of KikGR, we determined the structures of both the green and red state at 1.55 Å resolution. The double bond between His^{62}-C_α and His^{62}-C_β in the red chromophore is in a *cis* configuration, indicating that rotation along the His^{62} C_α-C_β bond occurs following cleavage of the His^{62} N_α-C_α bond. This structural rearrangement provides evidence that the β-elimination reaction governing the green-to-red photoconversion of KikGR follows an E1 (elimination, unimolecular) mechanism.

INTRODUCTION

Green fluorescent protein (GFP) from *Aequorea victoria* and GFP-like proteins allow direct genetic encoding of fluorescence; therefore, these proteins are widely used to monitor complex processes throughout molecular and cellular biology (Tsien, 1998; Miyawaki, 2005). The fluorescence of some of these proteins can be photomodulated by illumination at specific wavelengths (Patterson, 2008), thus enabling individual cells, organelles, or proteins to be labeled and followed with high spatiotemporal resolution. Another promising application of these photomodulable proteins is their use in super-resolution microscopy, such as photoactivated localization microscopy, stochastic optical reconstruction microscopy, and fluorescence photoactivated localization microscopy (Betzig et al., 2006; Rust et al., 2006; Hess et al., 2006; Geisler et al., 2007; Flors et al., 2007), in which a fluorescence image is constructed by using stochastic photoactivation and subsequent high-accuracy localization of individual fluorescent molecules.

Several photochemical processes are at work in the photoactivation behavior exhibited by fluorescent proteins. For example, the excitation peak at 504 nm is drastically enhanced after irradiation at ~400 nm in photoactivatable GFP (Patterson and Lippincott-Schwartz, 2002). This photoactivation involves decarboxylation of Glu^{222} and is thus irreversible. In contrast, reversible on-and-off switching of green fluorescence (518 nm) can be achieved using Dronpa (Ando et al., 2004) with light at ~400 nm (on) and ~490 nm (off). In Dronpa, light-dependent protonation/deprotonation and structural flexibility of the chromophore are responsible for the reversible switching (Mizuno et al., 2008).

Kaede (Ando et al., 2002), a natural fluorescent protein found in the stony coral *Trachyphyllia geoffroyi*, irreversibly changes its emission wavelength from green (518 nm) to red (582 nm) upon irradiation at ~400 nm. This large shift in emission wavelength enables high contrast in fluorescence highlighting; specifically, there is a 2000-fold increase in the red-to-green ratio that accompanies the shift. Another example of a natural photoconvertible fluorescent protein is EosFP (Wiedenmann et al., 2004) found in the coral *Lobophyllia hemprichii*. Furthermore, KikGR (Tsutsui et al., 2005), an engineered protein derived from KikG, a natural green-emitting fluorescent protein found in *Favia favus*, also undergoes green-to-red photoconversion. In all of these photoconvertible fluorescent proteins, a unique tripeptide, His^{62}-Tyr^{63}-Gly^{64}, forms a green chromophore that can be photoconverted to a red one. It has been shown that this process occurs via a β-elimination reaction that causes cleavage of the His^{62} N_α-C_α bond and the subsequent extension of a π-conjugated system (Mizuno et al., 2003; Nienhaus et al., 2005; Hayashi et al., 2007). Mutagenesis studies have revealed that the first His^{62} is required, but not sufficient, for the photo-induced β-elimination reaction, which also requires a specific three-dimensional structure (Mizuno et al., 2003). It should be noted that the cleavage of the His^{62} N_α-C_α bond releases a carboxamide-containing peptide as a leaving group, which is rarely seen in a conventional β-elimination reaction. The molecular mechanism that makes this reaction possible has remained unclear. Although X-ray crystallography, NMR, and mass spectroscopy were used to compare chromophore structures before and after the reaction, these analyses did not probe the nature and structure of intermediate states during the reaction directly.

In general, there are two basic mechanisms for an elimination reaction: E2 (elimination, bimolecular) and E1 (elimination,

unimolecular) (see Figure S1 available online). In the E2 elimination reaction, abstraction of a proton by a base and loss of the neighboring leaving group occur simultaneously, in a concerted manner, thus yielding a single product with a single isomeric configuration. Since the abstraction of a proton is a major driving force for the E2 mechanism, a strong base is generally required to initiate the reaction. In the E1 mechanism, in contrast, loss of the leaving group occurs first, resulting in formation of a carbocation intermediate. At that stage on the reaction pathway, structural rearrangement can occur on the carbocation intermediate, yielding a product with a different isomeric configuration. Next, the neighboring proton is abstracted in the final step of the reaction. Thus, the E1 reaction does not require a strong base.

In the red chromophores of both Kaede and EosFP, the C = C double bond between His^{62}-C_α and His^{62}-C_β assumes a *trans* configuration (Mizuno et al., 2003; Nienhaus et al., 2005; Hayashi et al., 2007). A reaction model based on the E2 mechanism has been proposed for the β-elimination of EosFP (Nienhaus et al., 2005), in which Glu^{212} acts as a base to abstract a proton. In the present study, we compared the crystal structures of a variant of KikGR in its green and red states. Despite similarity among the green chromophores of all the three photoconvertible fluorescent proteins, the red chromophore of the KikGR variant possessed the C = C double bond between His^{62}-C_α and His^{62}-C_β in a *cis* configuration, which indicates that the carbocation intermediate undergoes a structural rearrangement. Here we propose an E1-based reaction model that may comprehensively explain structural data for photoconversion of KikGR as well as rationalize some outstanding inconsistencies in explanation of the photoconversion mechanism of Kaede and EosFP.

RESULTS

KikGRX, a Crystalizable Variant of KiKGR

Whereas KikG, the original green-emitting fluorescent protein, was easily crystallized with sodium chloride as a precipitant, KikGR proved to be harder to crystallize. Thus, we screened a pool of KikGR mutants for one that formed well-diffracting crystals in both its green and red states. In addition, the pH sensitivity of the green state of the KikGR mutant was an important factor for examination of the β-elimination reaction kinetics because only excitation of the protonated form of the green chromophore leads to photoconversion. Therefore, the desirable KikGR mutant had to display high pK_a value in the green state. We isolated a KikGR mutant that met the above conditions. Although the isolated mutant KikGR contained four residue substitutions, L12M, E70K, P144S, and Q198L, it remained photoconvertible and crystallized in both the green and red states when sodium chloride was used as a precipitant. The mutant was named "KikGRX." The amino acid sequence alignments of KikG, KikGR, and KikGRX is shown in Figure 1A. KikGRX was photoconverted as efficiently as KikGR (Figures 1B and 1C and Table 1). The performance of KikGRX as an optical highlighter was also confirmed in mammalian cells (Figure S2). The absorption spectra of the protein at pH 7.0 in both the green and red states were identical to those of KikGR (Table 1). Of particular importance was the high pK_a value (8.0) of KikGRX in its green state (Table 1). As a result, about 80% of green KikGRX

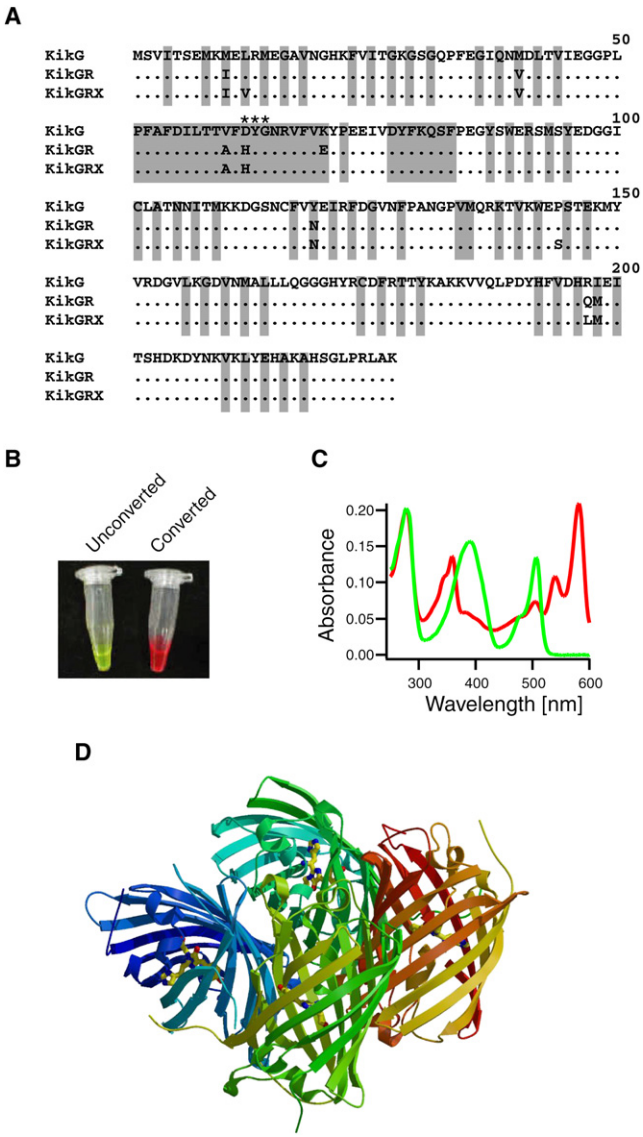

Figure 1. Generation and Characterization of KikGRX

(A) Amino acid sequence alignment of KikG, KikGR, and KikGRX. The residues forming the interior of the β barrel fold are shaded. Asterisks indicate those residues responsible for chromophore synthesis.

(B) Samples of the green-emitting (unconverted) and red-emitting (converted) states of KikGRX.

(C) Absorption spectra of KikGRX in the green-emitting (unconverted, green line) and red-emitting (converted, red line) states at pH 7.0.

(D) Tetrameric structure of KikGRX in the green state generated by crystallographic symmetry. The chromophores within the β barrel are shown as ball-and-stick representations.

in a crystal prepared at pH 7.0 was the protonated form of the protein.

Crystal Structures of Green and Red KikGRX

The overall folding schemes of KikGRX in the green and red states were identical to those of both *Aequorea* GFP (Örmo et al., 1996; Yang et al., 1996) and DsRed (Wall et al., 2000; Yarbrough et al., 2001) and other previously characterized GFP-like

Table 1. Spectroscopic Properties of KikG and Its Variants

KikG Variant	ε1(×10^3[M^{-1}cm^{-1}])	ε2(×10^3[M^{-1}cm^{-1}])	ϕ_{FL}	ϕ_{PC}(×10^{-3})	pK$_a$
KikG	81.0 (507 nm)		0.68 (480 nm)	0	4.2
KikGR (green-emitting)	25.8 (507nm)	15.6 (390 nm)	0.70 (480 nm)	4.7	7.8
KikGRX (green-emitting)	20.3 (507nm)	20.8 (390 nm)	0.70 (480 nm)	3.5	8
KikGR (red-emitting)	30.1 (583 nm)	21.0 (359 nm)	0.65 (540 nm), 0.92 (359 nm)		5.5
KikGRX (red-emitting)	28.6 (583nm)	18.6 (359nm)	0.65 (540 nm), 0.95 (359 nm)		5.7

ε, molar extinction coefficient for wavelength in parentheses at pH 7.0; ϕ_{FL}, fluorescence quantum yield for excitation at wavelength in parentheses; ϕ_{PC}, photoconversion quantum yield.

proteins, including KikG (Tsutsui et al., 2005). It features an 11 stranded β can with a central α helix holding a chromophore derived from a His^{62}-Tyr^{63}-Gly^{64} tripeptide. For both states, crystallographic symmetry generated a tetrameric structure (Figure 1D) similar to that seen for DsRed. Inter-β-can arrangements were indistinguishable between the two states; the root-mean-square deviation between the backbones of the crystallographic dimers was as small as 0.55 Å (Figure S3).

However, the structures within and near the chromophore clearly differed between the green and red states. While an unambiguous electron density connecting the His^{62}-C$_\alpha$ and His^{62}-N$_\alpha$ was present in the green state (Figure 2A, green arrows), it was obviously absent from the red state (Figure 2B, red arrows), indicating that a peptide cleavage had taken place. Stereographic views of the structures are also shown in Figure S4. The electron density map demonstrated that the red chromophore was composed of 5-(4-hydroxy-benzylidene)-2-[2-(1H-imidazol-4-yl)-vinyl]-3,5-dihydro-imidazol-4-one, which would be created by cleavage between His^{62}-C$_\alpha$ and His^{62}-N$_\alpha$ via a β-elimination reaction with a carboxamide leaving group.

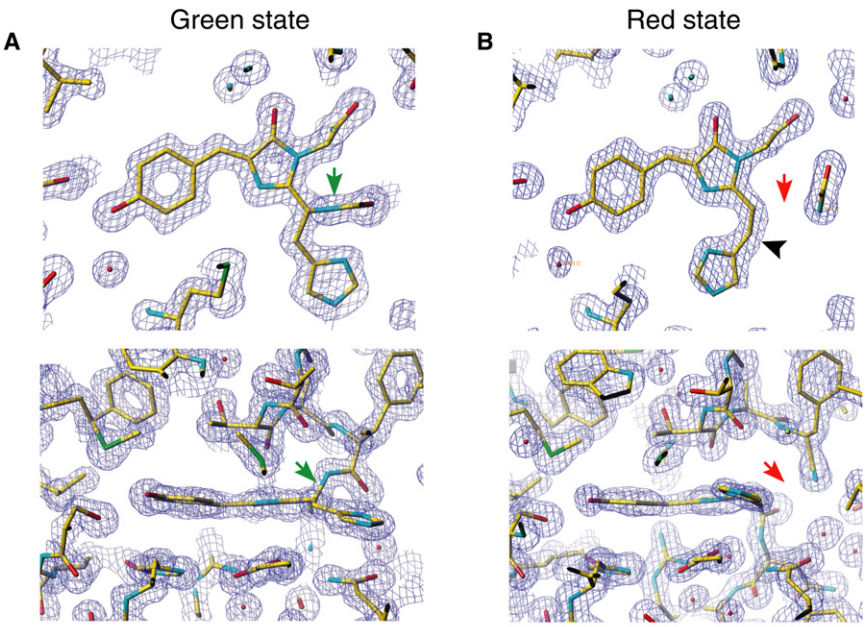

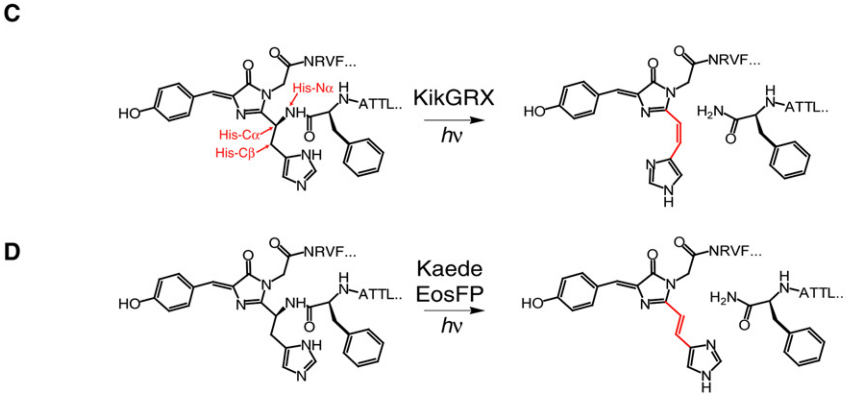

Figure 2. Structural Basis for the Green-to-Red Conversion

(A) Electron density maps (2Fo – Fc at 1.5 σ) showing the chromophore structure of the green-emitting (unconverted) state viewed from the top (top panel) and side (bottom panel) of the chromophore plane.

(B) The structure of the red (converted) state viewed from the top (top panel) and side (bottom panel) of the chromophore plane. Electron density connecting His^{62}-C$_\alpha$ and His^{62}-N$_\alpha$ exists in (A) (green arrows), but not in (B) (red arrows). The arrowhead indicates the *cis* configuration of the C = C double bond in the (5-imidazolyl)ethenyl group of the red-emitting chromophore.

(C and D) Summary of β-elimination and extension of the π-conjugated system in KikGRX (C) or Kaede and EosFP (D). The structures derived from Phe^{61}, His^{62}, Tyr^{63}, and Gly^{64} are drawn; the neighboring amino acids (single-letter code) are also shown. C = C double bonds in the (5-imidazolyl)ethenyl group and the neighboring bonds are colored in red in chromophores of the red states.

This is the same mechanism as that suggested for Kaede by crystallography (Hayashi et al., 2007) as well as mass spectrometry and NMR analyses (Mizuno et al., 2003), and that seen by crystallography for EosFP (Nienhaus et al., 2005).

Rearrangement of His^{62}, Evidence for a Reaction Intermediate

A remarkable change was observed in the red KikGRX structure. The red-emitting chromophore possessed a *cis* C = C double bond in the (5-imidazolyl)ethenyl group (Figure 2B, top, arrowhead; and Figure 2C). A comparison of Figure 2A (top) and Figure 2B (top) indicates that the imidazole ring rotates along the His^{62} C_α-C_β bond following peptide cleavage. This result differs from that seen for Kaede (Mizuno et al., 2003) and EosFP (Nienhaus et al., 2005), in which the cleavage leads to the formation of a *trans* double bond between His^{62}-C_α and His^{62}-C_β (Figure 2D).

The red-emitting chromophores of *cis* and *trans* isomers are spectroscopically distinguishable. First, we denatured KikGRX and Kaede in SDS. After exposure to SDS, the chromophore was no longer fluorescent, but retained an absorption spectrum that reflected the chromophore structure. While the green chromophores of KikGRX and Kaede exhibited identical absorption spectra that both peaked at 441 nm (Figures 3A and 3B), the red chromophores of KikGRX (a *cis* isomer) and Kaede (a *trans* isomer) displayed distinct absorption spectra with maxima at 512 (Figure 3A) and 496 (Figure 3B) nm, respectively. When compared, the spectra of the green and red chromophores of KikGR were identical (Figure 3C) to those for KikGRX (Figure 3A).

Reaction Mechanisms for Green-to-Red Photoconversion

Our crystallographic data demonstrated that the imidazole ring of His^{62} flipped around in KikGRX compared to Keade and EosFP. This structural rearrangement provides evidence that the β-elimination reaction leading to the green-to-red photoconversion proceeds by the E1 mechanism. Figure 4 shows our model of the sequential reactions for the photoconversion of KikGR(X) versus Kaede and EosFP. In the green state, the imidazole ring of His^{62} is stabilized by hydrogen bonding between N_δ of His^{62} and O of Phe^{61} (Figure 4A). With the phenolic hydroxyl group in its protonated state, the chromophore is excited (Figure 4B). Next, excited-state proton transfer occurs, resulting in ionization of the phenolic hydroxyl group (Figure 4C). In *Aequorea* GFP, the side chain of Glu^{222} residue in the hydrogen bond network acts as a transient proton acceptor (Tsien, 1998); however, we did not identify any potential proton acceptor residues in the green KikGRX structure that directly interacted with the phenolic hydroxyl group of the chromophore. The His^{62} imidazole group has been proposed to receive the proton, possibly via weak hydrogen-mediated interactions (Figure 4C). Photoexcitation promotes cleavage of the N_α-C_α bond of His^{62} through two mechanisms (Figure 4D). First, the excited ionized phenolic hydroxyl group donates electrons to the π-conjugated system. Second, the protonated imidazole ring of His^{62} acts as an acid, protonating the carboxamide group. Cleavage generates a hybrid of the two structures (Figure 4E). This resonance stabilizes the intermediate species, as seen for the carbocation in the

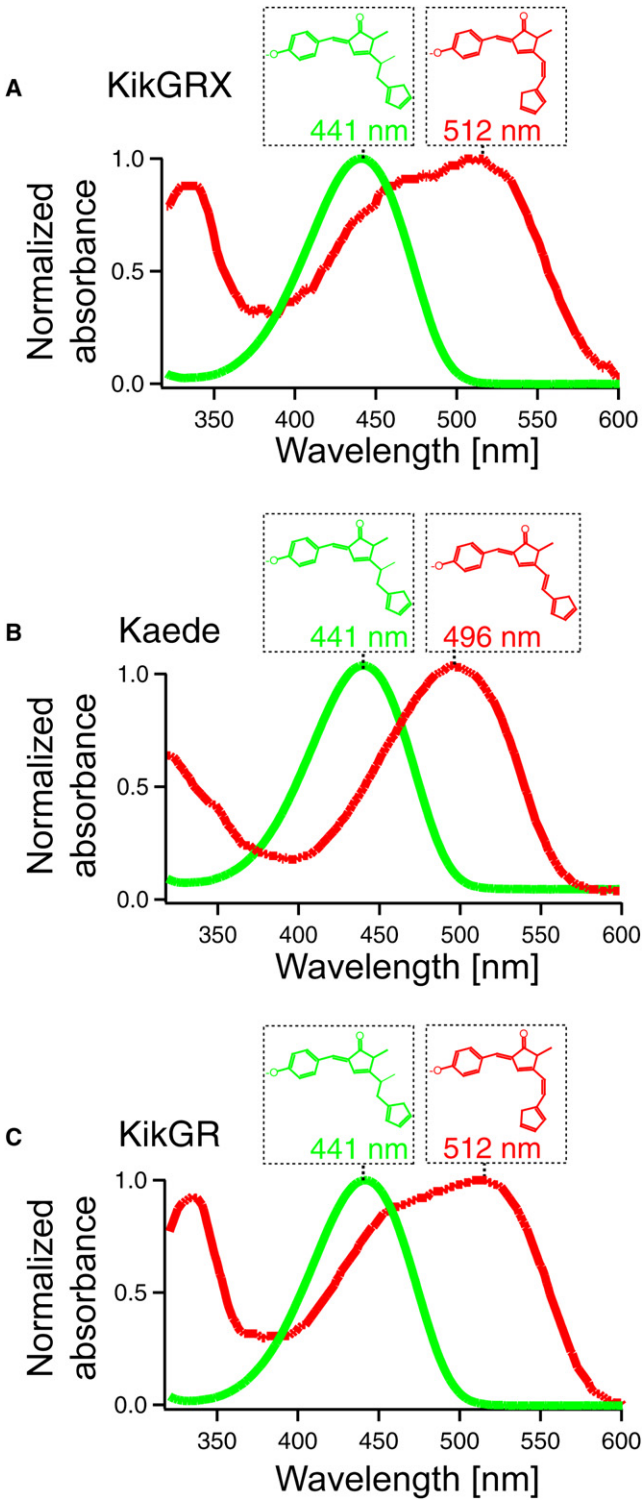

Figure 3. Spectral Fingerprints of the Green and Red Chromophore Species

Absorption spectra of denatured KikGRX (A), Kaede (B), and KikGR (C) in the green (green line) and red (red line) states. The absorption maxima are shown with the corresponding chromophore structures.

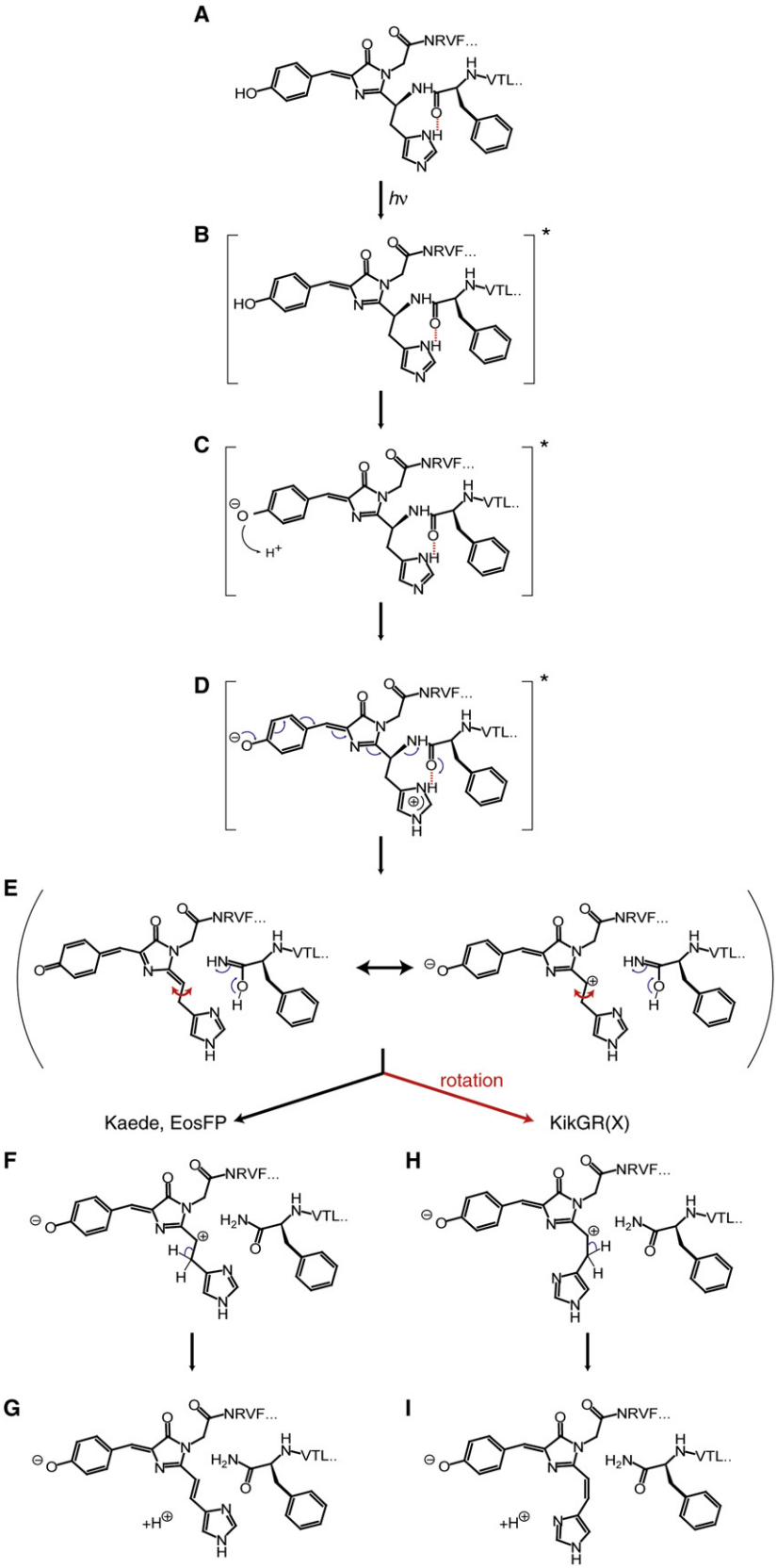

Figure 4. E1 Reaction Model for the Green-to-Red Photoconversion of Fluorescence Proteins

Structures derived from Phe[61], His[62], Tyr[63], and Gly[64] are drawn; the neighboring amino acids (single-letter code) are also shown.

(A) The green chromophore in the initial protonated state.

(B) Excitation of the chromophore by ultraviolet light.

(C) Excited-state proton transfer.

(D) The excited ionized phenolic hydroxyl group and protonated imidazole ring of His[62].

(E) Resonance stabilization of the intermediate structure. Allowed rotation of the imidazole ring along the bond between His[62]-C_α and His[62]-C_β is indicated by red arrows. The leaving group is carboxamidic acid, which becomes carboxamide through tautomerization.

(F and H) Tautomerization with (H) and without (F) rotation of the imidazole ring.

(G and I) Loss of a proton from C_β leads to completion of the red chromophore with either a *trans* (G) or *cis* (I) double bond.

E1 elimination reaction. At this point, the hydrogen-bonding interaction between N_δ of His^{62} and O of Phe^{61} is disrupted, permitting free rotation of the imidazole along the axis between His^{62}-C_α and His^{62}-C_β (Figure 4E). Thus, the ring flips around in KikGR(X) (Figure 4H), while it does not in Kaede or EosFP (Figure 4F). This decision may depend on the cavity structure of the fluorescent protein. In each case, a proton is lost from His^{62}-C_β, leading to production of a *trans* or *cis* C = C double bond within the (5-imidazolyl)ethenyl group (Figure 4G or 4I, respectively).

DISCUSSION

It should be noted that all photomodulable fluorescent proteins described thus far carry histidine residues within or near the chromophore. Histidine, however, appears to play different roles depending on whether it is situated outside the chromophore (photoactivatable GFP and KFP1) or within the chromophore (Kaede, EosFP, and KikGR(X)). To explore the active involvement of histidine residues within the chromophore in photochemical reactions, we studied the X-ray structures of a crystallizable variant of KikGR (KikGRX). Importantly, the green form of KikGRX (green KikGRX) exhibited a high pK_a value (8.0). Therefore, when crystallized at pH 7.0, the molecule existed principally in its protonated form. Because the acid-induced protonated form is responsible for the photoconversion, the crystal structure of green KikGRX provides direct information about the roles of His^{62} in the photochemical reaction. In contrast, green EosFP (pK_a = 5.8) and green Kaede (pK_a = 5.6) were crystallized at pH 8.5 (Nienhaus et al., 2005) and pH 8.0 (Hayashi et al., 2007), respectively, and were mostly in their ionized forms and not poised for photoconversion. Although clear hydrogen-bonding networks have not been identified in the green KikGRX structure determined at 1.55 Å, it is likely that the excited-state proton transfer at the hydroxyl group is coupled with the protonation of the carboxyamide leaving group. His^{62} may play critical roles in these processes by serving as a relay point during the proton transfer. The high resolution of the crystal structure allowed the nitrogen (N) atoms in the heterocyclic rings to be clearly identifiable (Figure S5); N_δ and N_ε of His^{62} were assigned to high electron density positions in the imidazole ring of His^{62} in both molecules within the asymmetrical unit. This orientation provides a geometry that allows for the favorable interaction of the N_δ of His^{62} and the O of Phe^{61} via hydrogen bonding. This hydrogen-bonding interaction is important because it stabilizes the imidazolium ring of His^{62} and also allows His^{62} to supply a proton to the carboxamide leaving group.

Before photoconversion, in the green form, KikGRX has a chromophore conformation similar to EosFP (Figure S6B) and Kaede (Figure S6C). One potentially important difference is that a well-defined water molecule can be seen in the proximity of the His^{62} imidazole in green forms of Kaede and EosFP, but not in the green KikGRX. The present study demonstrates that KikGR(X) differs from Kaede and EosFP in that the photoconversion of KikGR(X) results in a flipping of the His^{62} imidazole ring. As a result, the double bond between His^{62}-C_α and His^{62}-C_β is in a *cis* configuration in the red KikGR(X) chromophore.

The emission wavelength of the red chromophore with the *cis* configuration (593 nm) is longer than the emission wavelength of the *trans*-configured red Kaede (582 nm) and EosFP (581 nm). Other natural photoconvertible fluorescent proteins in their red forms show similar emission maxima as Kaede and EosFP; mcavRFP and rfloRFP emit fluorescence at 580 and 574 nm, respectively (Labas et al., 2002). Therefore, the red chromophores of mcavRFP and rfloRFP are also likely to be *trans* isomers. Apparently, the *cis* configuration of red chromophores is energetically less stable than the *trans* configuration. Thus, it is interesting that the in vitro evolution of KikG in our previous study created a β-can cavity that stabilizes the *cis* isomer of the chromophore. KikGR(X) may be practically superior to Kaede or EosFP, in that the photoconverted KikGR(X) emits fluorescence at a longer wavelength (593 nm) than the photoconverted Kaede (582 nm) or EosFP (581 nm), whereas their green emissions are indistinguishable (516 or 517 nm). This larger wavelength shift may permit more efficient separation between the green and red fluorescence emissions.

A previous X-ray structure analysis of the green and red states of EosFP led to the proposal that the β-elimination for the photoconversion was governed by an E2 mechanism (Nienhaus et al., 2005) (Figure S7). In this model, a glutamate residue (Glu^{212}) (corresponding to Glu^{214} in KikGR(X)) functions as a base during the photoconversion of EosFP. The base abstracts a proton from His^{62}-C_β; simultaneously, a carboximidic acid separates due to the cleavage of the N_α-C_α bond of His^{62}. However, there are some unresolved issues surrounding the proposed E2 mechanism. First, as was pointed out by Nienhaus et al. (2005), it does not explain why the green chromophore must be in its protonated state in order to undergo excitation and photoconversion. Second, according to the proposed model, the red chromophore of KikGRX would be expected to have a *trans* C = C double bond between His^{62}-C_α and His^{62}-C_β, which is not consistent with our observations. As the E2 mechanism excludes structural rearrangements, and since we clearly see evidence for rearrangement in our structure, we base our KikGRX model on the E1 mechanism. This model accounts for the capacity of carboxamide to serve as a leaving group in the β-elimination reaction and accounts for both the *trans* and *cis* C = C double bonds in the (5-imidazolyl)ethenyl group of red chromophores. We also propose that photoconversion in EosFP and Kaede might also follow the E1 reaction mechanism, but that remains to be formally confirmed by future experimental work. Nonetheless, we believe that our study presents a general scheme for photochemistry grounded in the theory of organic chemical reactions as we demonstrate that photoconvertible fluorescent proteins use a remarkable reaction mechanism in which photoexcitation and β-elimination are intricately coupled.

SIGNIFICANCE

Understanding the molecular mechanisms of photomodulable fluorescent proteins enables scientists to design photoconvertible proteins with desirable properties. KikGR is a fluorescent protein engineered to display green-to-red photoconvertibility upon induction by irradiation with ultraviolet or violet light. Similar to Kaede and EosFP, two naturally occurring photoconvertible proteins, KikGR contains a His^{62}-Tyr^{63}-Gly^{64} tripeptide sequence, which forms a green chromophore that can be photoconverted to a red one via

formal β-elimination and subsequent extension of the π-conjugated system. Using a crystallizable variant of KikGR, we determined the structures of both the green and red states at 1.55 Å resolution. The double bond between His^{62}-C_α and His^{62}-C_β in the red chromophore is in a *cis* configuration, indicating that rotation along the His^{62} C_α-C_β bond occurs following cleavage of the His^{62} N_α-C_α bond. The combination of this structural rearrangement with the requirement for the green chromophore to be in its protonated form for photoexcitation provides evidence that the β-elimination reaction governing the green-to-red photoconversion of KikGR follows an E1 (elimination, unimolecular) mechanism. Importantly, this mechanism also occurs during the conversion of Kaede and EosFP. Furthermore, the requirement for the green chromophore to be in its protonated form for green-to-red photoconversion implies an intricate coupling between photoexcitation and β-elimination reactions. Thus, the β-elimination reaction here occurs via use of carboxamide as a leaving group, which is not typically seen in conventional β-elimination reactions.

EXPERIMENTAL PROCEDURES

Protein Expression, Purification, Spectroscopy, and Crystallization

Protein expression in *Escherichia coli* (strain: JM109DE3) and purification by Ni^{2+} affinity chromatography were performed as described previously (Ando et al., 2002). Absorption/fluorescence spectroscopy and pH titrations were performed at room temperature as previously described (Ando et al., 2002). Quantum efficiencies for photoconversions were measured as described previously (Tsutsui et al., 2005). For spectral finger printing of chromophore, protein was denatured with 1% SDS in 0.2 M NaOH. For crystallization, the protein was further purified on a cation exchange column (MonoQ; GE Healthcare) driven by the AKTA-HPLC system (GE Healthcare), and then concentrated to ~30 mg/ml in 10 mM NaCl and 10 mM Tris-HCl (pH 9.0) by filtration (Vivaspin; Vivascience). The protein solution, mixed with an equal volume of a crystallization mother liquid [4.0 M NaCl and 0.1 M HEPES-NaOH (pH 7.0)], was microseeded and crystallized by sitting-drop vapor diffusion. Crystals were grown for several days at 20°C, soaked in a cryoprotectant [20% v/v glycerol, 4.0 M NaCl, and 0.1 M HEPES-NaOH (pH 7.0)], and flash-frozen in a 100 K N_2 gas stream before data collection.

Crystal Structure Determination

Diffraction data from a single crystal were collected at Beamline 44B2 in the SPring-8 Center. The data were processed with the HKL2000 software (Otwinowski and Minor, 1997). The crystals belong to space group C2, with two molecules in the asymmetrical unit. The unit cell dimensions were as follows: a = 97 Å; b = 119 Å; c = 49 Å; β = 120°. The statistics for crystals analyzed in this study are summarized in Table 2. Phasing was carried out with CNS (Brünger et al., 1998). Graphical modeling was performed with TURBO-FRODO (Roussel and Cambillau, 1989). Radiated crystals were re-dissolved after data collection to test spectral properties, which did not differ from those of fresh protein solution (data not shown).

ACCESSION NUMBERS

Coordinates have been deposited in the Protein Data Bank with accession codes 2DDD (KikGRX; green state) and 2DDC (KiKGRX; red state).

SUPPLEMENTAL DATA

Supplemental Data include seven figures and can be found with this article online at http://www.cell.com/chemistry-biology/supplemental/S1074-5521(09)00361-5.

Table 2. Data Collection and Refinement Statistics

	Green State	Red State
PDB Code	2DDD	2DDC
Data collection statistics		
Space group	C2	C2
Wavelength (Å)	1.0	0.7
Unit cell dimensions (Å)	a = 96.8; b = 118.4; c = 48.8; β = 119.96°	a = 97.4; b = 118.3; c = 49.4; β = 120.44°
Resolution range (Å)[a]	100–1.55 (1.62–1.55)	100–1.55 (1.62–1.55)
Number of observations	242,266	452,761
Number of unique reflections	69,780	69,163
R_{sym} (%)[a]	4.1 (26.7)	4.9 (15.6)
Mean I / σ (%)[a]	27.6 (4.1)	23.3 (6.8)
Completeness (%)[a]	99.7 (99.1)	97.9 (84.6)
Redundancy[a]	3.5 (3.0)	6.2 (4.2)
Refinement statistics		
Resolution range for refinement (Å)	100–1.55	100–1.55
R_{work} (%)	17.8	19.0
R_{free} (%)	19.5	21.2
Rmsd from ideal		
Bond length (Å)	0.005	0.011
Bond angle (°)	1.4	1.5
Average B factor (Å^2)	14.2	20.1
Number of water molecules	600	559
Ramachandran plot (%)		
Favored	94.2	92.4
Allowed	5.8	7.6
Generously allowed	0	0
Disallowed	0	0

[a] Values in parentheses are for the highest-resolution shell.

ACKNOWLEDGMENTS

This work was supported by grants from the Special Postdoctoral Researcher Program of RIKEN to H.T. and the Molecular Ensemble Development Research Team, the Special Coordination Fund for the promotion of the Ministry of Education, Culture, Sports, Science and Technology of Japan, the New Energy and Industrial Technology Development Organization, and the Human Frontier Science Program to A.M. The authors would like to thank R. Kato and R. Noyori for valuable advice.

Received: August 2, 2009
Revised: October 15, 2009
Accepted: October 16, 2009
Published: November 24, 2009

REFERENCES

Ando, R., Hama, H., Yamamoto-Hino, M., Mizuno, H., and Miyawaki, A. (2002). An optical marker based on the UV-induced green-to-red photoconversion of a fluorescent protein. Proc. Natl. Acad. Sci. USA *99*, 12651–12656.

Ando, R., Mizuno, H., and Miyawaki, A. (2004). Regulated fast nucleocytoplasmic shuttling observed by reversible protein highlighting. Science *306*, 1370–1373.

Betzig, E., Patterson, G.H., Sougrat, R., Lindwasser, O.W., Olenych, S., Bonifacino, J.S., Davidson, M.W., Lippincott-Schwartz, J., and Hess, H.F. (2006). Imaging intracellular fluorescent proteins at nanometer resolution. Science *313*, 1642–1645.

Brünger, A.T., Adams, P.D., Clore, G.M., DeLano, W.L., Gros, P., Grosse-Kunstleve, R.W., Jiang, J.S., Kuszewski, J., Nilges, M., Pannu, N.S., et al. (1998). Crystallography & NMR system: A new software suite for macromolecular structure determination. Acta Crystallogr. D. Biol. Crystallogr. *54*, 905–921.

Flors, C., Hotta, J., Uji-I, H., Dedecker, P., Ando, R., Mizuno, H., Miyawaki, A., and Hofkens, J. (2007). A stroboscopic approach for fast photoactivation-localization microscopy with Dronpa mutants. J. Am. Chem. Soc. *129*, 13970–13977.

Geisler, C., Schönle, A., von Middendorf, C., Bock, H., Eggeling, C., Egner, A., and Hell, S.W. (2007). Resolution of lambda/10 in fluorescence microscopy using fast single molecule photo-switching. Appl. Phys. A *88*, 223–226.

Hayashi, I., Mizuno, H., Tong, K.I., Furuta, T., Tanaka, F., Yoshimura, M., Miyawaki, A., and Ikura, M. (2007). Crystallographic evidence for water-assisted photo-induced peptide cleavage in the stony coral fluorescent protein kaede. J. Mol. Biol. *372*, 918–926.

Hess, S.T., Girirajan, T.P.K., and Mason, M.D. (2006). Ultra-high resolution imaging by fluorescence photoactivation localization microscopy. Biophys. J. *91*, 4258–4272.

Labas, Y.A., Gurskaya, N.G., Yanushevich, Y.G., Fradkov, A.F., Lukyanov, K.A., Lukyanov, S.A., and Matz, M.V. (2002). Diversity and evolution of the green fluorescent protein family. Proc. Natl. Acad. Sci. USA *99*, 4256–4261.

Mizuno, H., Mal, T.K., Tong, K.I., Ando, R., Furuta, T., and Miyawaki, A. (2003). Photo-induced peptide cleavage in the green-to-red conversion of a fluorescent protein. Mol. Cell *12*, 1051–1058.

Mizuno, H., Mal, T.K., Wälchli, M., Kikuchi, A., Fukano, T., Ando, R., Jeyakanthan, J., Taka, J., Shiro, Y., Ikura, M., and Miyawaki, A. (2008). Light-dependent regulation of structural flexibility in a photochromic fluorescent protein. Proc. Natl. Acad. Sci. USA *105*, 9227–9232.

Miyawaki, A. (2005). Innovations in the imaging of brain functions using fluorescent proteins. Neuron *48*, 189–199.

Nienhaus, K., Nienhaus, G.U., Wiedenmann, J., and Nar, H. (2005). Structural basis for photo-induced protein cleavage and green-to-red conversion of fluorescent protein EosFP. Proc. Natl. Acad. Sci. USA *102*, 9156–9159.

Örmo, M., Cubitt, A.B., Kallio, K., Gross, L.A., Tsien, R.Y., and Remington, S.J. (1996). Crystal structure of the Aequorea victoria green fluorescent protein. Science *273*, 1392–1395.

Otwinowski, Z., and Minor, W. (1997). Processing of X-ray diffraction data collection in oscillation mode. Methods Enzymol. *276*, 307–326.

Patterson, G.H. (2008). Photoactivation and imaging of photoactivatable fluorescent proteins. Curr. Protoc. Cell Biol. *21*:Unit 21.6.

Patterson, G.H., and Lippincott-Schwartz, J. (2002). A photoactivatable GFP for selective photolabeling of proteins and cells. Science *297*, 1873–1877.

Roussel, A., and Cambillau, C. (1989). Silicon Graphics Geometry Partner Directory (Mountain View, CA: Silicon Graphics), pp. 77–78.

Rust, M.J., Bates, M., and Zhuang, X.W. (2006). Sub-diffraction-limit imaging by stochastic optical reconstruction microscopy (STORM). Nat. Methods *3*, 793–795.

Tsien, R.Y. (1998). The green fluorescent protein. Annu. Rev. Biochem. *67*, 509–544.

Tsutsui, H., Karasawa, S., Shimizu, H., Nukina, N., and Miyawaki, A. (2005). Semi-rational engineering of a coral fluorescent protein into an efficient highlighter. EMBO Rep. *6*, 233–238.

Wall, M.A., Socolich, M., and Ranganathan, R. (2000). The structural basis for red fluorescence in the tetrameric GFP homolog DsRed. Nat. Struct. Biol. *7*, 1133–1138.

Wiedenmann, J., Ivanchenko, S., Oswald, F., Schmitt, F., Röcker, C., Salih, A., Spindler, K.D., and Nienhaus, G.U. (2004). EosFP, a fluorescent marker protein with UV-inducible green-to-red fluorescence conversion. Proc. Natl. Acad. Sci. USA *101*, 15905–15910.

Yang, F., Moss, L.G., and Phillips, G.N., Jr. (1996). The molecular structure of green fluorescent protein. Nat. Biotechnol. *14*, 1246–1251.

Yarbrough, D., Wachter, R.M., Kallio, K., Matz, M.V., and Remington, S.J. (2001). Refined crystal structure of DsRed, a red fluorescent protein from coral, at 2.0-Å resolution. Proc. Natl. Acad. Sci. USA *98*, 462–467.